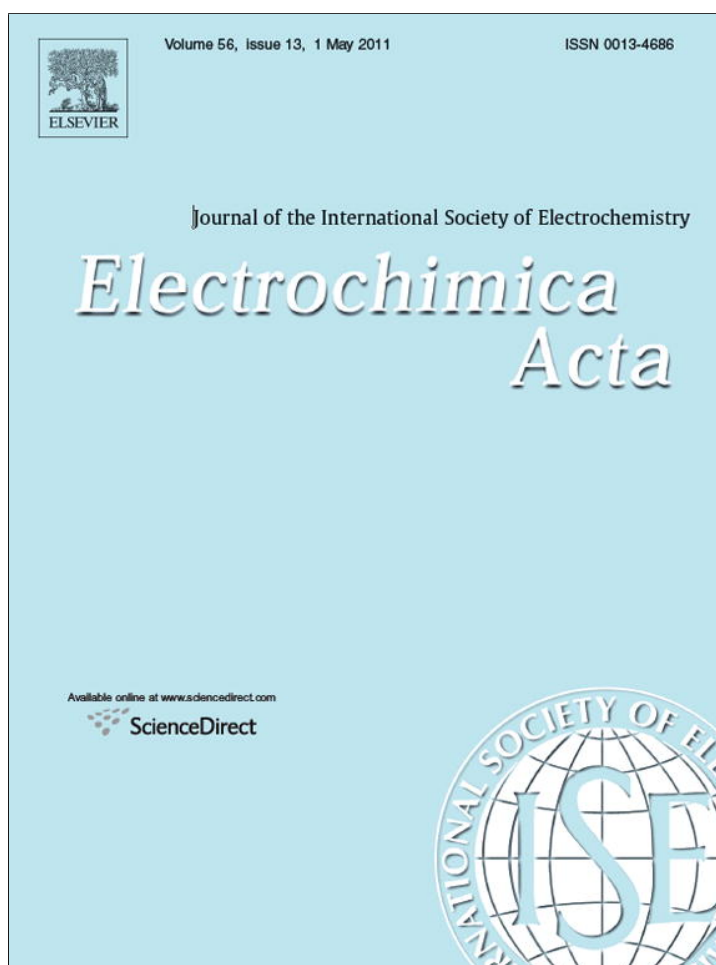


Provided for non-commercial research and education use.
Not for reproduction, distribution or commercial use.



This article appeared in a journal published by Elsevier. The attached copy is furnished to the author for internal non-commercial research and education use, including for instruction at the authors institution and sharing with colleagues.

Other uses, including reproduction and distribution, or selling or licensing copies, or posting to personal, institutional or third party websites are prohibited.

In most cases authors are permitted to post their version of the article (e.g. in Word or Tex form) to their personal website or institutional repository. Authors requiring further information regarding Elsevier's archiving and manuscript policies are encouraged to visit:

<http://www.elsevier.com/copyright>



Contents lists available at ScienceDirect

Electrochimica Acta

journal homepage: www.elsevier.com/locate/electacta

Gold nanoparticles/water-soluble carbon nanotubes/aromatic diamine polymer composite films for highly sensitive detection of cellobiose dehydrogenase gene

Guangming Zeng^{a,b,*}, Zhen Li^{a,b}, Lin Tang^{a,b}, Mengshi Wu^{a,b}, Xiaoxia Lei^{a,b}, Yuanyuan Liu^{a,b}, Can Liu^{a,b}, Ya Pang^{a,b}, Yi Zhang^{a,b}

^a College of Environmental Science and Engineering, Hunan University, Changsha 410082, PR China

^b Key Laboratory of Environmental Biology and Pollution Control (Hunan University), Ministry of Education, Changsha 410082, PR China

ARTICLE INFO

Article history:

Received 1 December 2010

Received in revised form 11 March 2011

Accepted 11 March 2011

Available online 17 March 2011

Keywords:

Gold nanoparticles

Water-soluble multiwalled carbon nanotubes

Poly (1,5-naphthalenediamine)

Cellobiose dehydrogenase gene

Electrochemical sensor

ABSTRACT

An electrochemical sensor based on gold nanoparticles (GNPs)/multiwalled carbon nanotubes (MWCNTs)/poly (1,5-naphthalenediamine) films modified glassy carbon electrode (GCE) was fabricated. The effectiveness of the sensor was confirmed by sensitive detection of cellobiose dehydrogenase (CDH) gene which was extracted from *Phanerochaete chrysosporium* using polymerase chain reaction (PCR). The monomer of 1,5-naphthalenediamine was electropolymerized on the GCE surface with abundant free amino groups which enhanced the stability of MWCNTs modified electrode. Congo red (CR)-functionalized MWCNTs possess excellent conductivity as well as high solubility in water which enabled to form the uniform and stable network nanostructures easily and created a large number of binding sites for electrodeposition of GNPs. The continuous GNPs together with MWCNTs greatly increased the surface area, conductivity and electrocatalytic activity. This electrode structure significantly improved the sensitivity of sensor and enhanced the DNA immobilization and hybridization. The thiol modified capture probes were immobilized onto the composite films-modified GCE by a direct formation of thiol–Au bond and horseradish peroxidase–streptavidin (HRP–SA) conjugates were labeled to the biotinylated detection probes through biotin–streptavidin bond. Scanning electron microscopy (SEM), electrochemical impedance spectroscopy (EIS) and cyclic voltammetry (CV) were used to investigate the film assembly and DNA hybridization processes. The amperometric current response to HRP-catalyzed reaction was linearly related to the common logarithm of the target nucleic acid concentration in the range of 1.0×10^{-15} – 1.0×10^{-10} M, with the detection limit of 1.2×10^{-16} M. In addition, the electrochemical biosensor exhibited high sensitivity, selectivity, stability and reproducibility.

© 2011 Elsevier Ltd. All rights reserved.

1. Introduction

In nature, lignocellulose accounts for the major part of biomass and, consequently, its degradation is essential for the operation of the global carbon cycle [1]. Biodegradation resistance of wood and other lignified materials is directly related to the presence of lignin [2]. The white-rot fungi *Phanerochaete chrysosporium*, one of the most effective lignin degraders, has become the model system for studying the physiology and genetics of lignin degradation which is currently understood as an enzymatic process [3,4]. Cellobiose dehydrogenase (CDH) is an extracellular enzyme which is believed to be involved in both cellulose and lignin degradation [5]. It is suggested that CDH can prevent product inhibition during cellulose

degradation by oxidizing cellobiose, and that it produces hydroxyl radicals through a Fenton-type reaction that can initiate depolymerization in lignin degradation [6]. At present, CDH has been purified and characterized from a large number of basidiomycete fungi, and the role, properties, and structure of the enzyme has been explained by many researchers [7–10]. Moreover, CDH activity was detected in some assays based on the reduction of benzoquinone or dichlorophenol indophenol [11–13]. A rapid and sensitive method for determining the specific CDH sequences from *P. chrysosporium* would provide a useful tool to gain a fuller understanding of the catalytic mechanisms and the biological roles proposed for CDH.

Electrochemical DNA biosensors with fast response, high sensitivity and low cost have received considerable attention in the fields of environment, biology, medicine, and food stuff [14–19]. The immobilization amount along with the accessibility of DNA probe for hybridization recognition is the most crucial issue faced with any DNA biosensor. Metal nanoparticles and carbon nanotubes (CNTs) can be used as the elegant nanomaterials for the control of DNA immobilization and provide good opportunities for sequence-

* Corresponding author at: College of Environmental Science and Engineering, Hunan University, Changsha 410082, PR China. Tel.: +86 731 88822754; fax: +86 731 88823701.

E-mail addresses: zgming@hnu.cn (G. Zeng), happylizhen@yeah.net (Z. Li).

Table 1
Sequences of oligonucleotide used in biosensor.

Oligonucleotide	Sequence (5'–3')
Capture probe	HS-(CH ₂) ₆ -TGTCAAAGTGGCAGTTCCTCCGT
Detection probe	CAGCGAGTGGAGGAAACAA-biotin
Target oligonucleotide	TGTGTTCTCCACTCGCTGTTTTTTTTTTTTTTTTTTTTTTTTTTTACGGGAACCTGCCACTTTGACA
Two-base-mismatched oligonucleotide	TGTGTTCTCCACTCAGTGTGTTTTTTTTTTTTTTTTTTTTTTTTTTTACGGGAACCTGCCACTTTGATA
Sense primer	ATTGTTCTCCACTCG
Anti-sense primer	CCGCCATGTTCCTCCACTC

specific target DNA detection [20–23]. Recently, gold nanoparticles (GNPs) are of great interest due to their large surface area and favorable biocompatibility in biosensing, diagnostics and molecular therapeutics [24,25]. Carbon nanotubes with unique electronic and mechanical properties have been widely applied in electroanalysis including protein electrochemistry and electrochemical biosensor [26–28]. Modification of electrode with nanoparticles and carbon nanotubes has been considered as an effective strategy to enhance the electrochemical sensitivity, biomolecular stability and sensor performance [29,30].

The combination of GNPs and CNTs which generated excellent electrocatalytic behavior has been immobilized on the electrode surface via various strategies, such as electrodeposition, sol-gel, noncovalent functionalization and covalent linking. Wang et al. constructed an electrochemical DNA sensor on the basis of GNPs, CNTs and zinc oxide nanowires (ZnONWs). Multi-walled carbon nanotubes (MWCNTs) were dispersed in anhydrous ethanol and cast on the ZnONWs-modified electrode surface, followed by the electrochemical deposition of gold nanoparticles [31]. Two electrochemical sensors were fabricated by electrodeposition of GNPs onto carbon nanotubes film pre-cast on a GCE [32] or on ionic liquid-MWCNT gel film coated GCE [33]. MWCNTs, GNPs and chitosan were integrated with the aid of ultrasonic agitation [34] or based on the direct redox reaction [35] to improve the sensitivity and capability of sensor. The composite of MWCNTs and Au colloids dispersed in *N,N'*-dimethylformamide (DMF) was dropped onto the surface of GCE to improve the electroactivity [36]. A new strategy for fabricating GNP/MWCNT nanohybrid through noncovalent functionalization of the MWCNTs with supramolecular surfactant was demonstrated [37]. Wang et al. synthesized MWCNT/thionine/Au composites with π - π stacking and electrostatic interactions [38]. Zhang et al. investigated a DNA biosensor built by layer-by-layer covalent attachment of GNPs and MWCNTs on an Au electrode [39]. The surface modification of GNPs integrated with MWCNTs could significantly increase the electroactive surface area as well as the synergistic electrocatalytic activity. However, the MWCNTs suspension was usually dispersed by ultrasonic agitation and immobilized on the electrode surface with a simple casting method. Therefore, it is difficult to distribute MWCNTs homogeneously and firmly to the electrode surface which greatly influenced the capability of biosensor. In order to overcome these drawbacks, a convenient and sensitive method was proposed by the introduction of water-soluble MWCNTs and poly (1,5-naphthalenediamine).

In this work, an electrochemical sensor based on GNPs/MWCNTs/poly (1,5-naphthalenediamine) films modified GCE was fabricated. Poly (1,5-naphthalenediamine), a conducting aromatic diamine polymer with good film-forming ability, was electropolymerized on the GCE surface. Congo red (CR)-functionalized water-soluble MWCNTs were uniformly and stably casted on the electrode with the covalent bond. The continuous GNPs were subsequently introduced to the modified electrode surface by electrodeposition. The nanocomposite films-modified electrode exhibited remarkable ability to increase the electroactive surface area and enhance the electron transfer rate, which significantly improved the sensitivity and selectivity of biosensor.

Consequently, the composite films-modified GCE was developed for the determination of cellobiose dehydrogenase gene extracted from *P. chrysosporium*. The electrochemical sensor was convenient and sensitive, and can be used for the detection of bioactive substances in life sciences, clinical medicine and environmental pollution control systems.

2. Experimental

2.1. Materials

MWCNTs (purity > 97 wt%, Nanotechnology Co., Ltd., USA) were synthesized by the catalytic pyrolysis method and used as received. 1,5-Naphthalenediamine was obtained from Johnson Matthey Co., Ltd. (USA) and horseradish peroxidase-streptavidin (HRP-SA) was from Dingguo Biotechnology Co., Ltd. (Beijing, China). Congo red and hydrogen tetrachloroaurate (HAuCl₄·4H₂O) were purchased from Shanghai Reagent Co., Ltd. (Shanghai, China). 1-Ethyl-3-(3-dimethyl aminopropyl) carbodiimide (EDC), N-hydroxysuccinimide (NHS), tris (hydroxymethyl) aminomethane (Tris) and 6-mercapto-1-hexanol (MCH) were from Sigma-Aldrich, (USA). All chemicals were of analytical grade quality, and all solutions were prepared in deionized water of 18 M Ω purified from a Milli-Q purification system. The oligonucleotide primers as well as target-specific probes were self-designed by Primer Premier 5.0, which were synthesized by Sangon (Shanghai, China). The sequences of oligonucleotide are shown in Table 1.

2.2. Apparatus

Electrochemical measurements were performed on a CHI660B electrochemistry system (Chenhua Instrument, Shanghai, China). The three-electrode system contained a glassy carbon (GCE, 3.0 mm in diameter) working electrode, a saturated calomel or Ag/AgCl reference electrode and a Pt wire counter electrode. The scanning electron microscopy (SEM) was obtained on Hitachi S-4800 (Japan). A UV-2250UV-vis spectrophotometer (Shimadzu, Japan), a CS501-SP thermostat (Huida Instrument, Chongqing, China) and a ZK-82 vacuum drying oven (Shanghai Instrument Co., China) were used in the assay. The PCR reaction was carried out in a Bio-Rad MyCycler (Bio-Rad Laboratories, USA) and the Gel electrophoresis analysis was in a DYY-7C electrophoresis system (Liuyi Instrument, Beijing, China). Gel images were captured on a Gel Doc 2000 imaging system (Bio-Rad Laboratories, USA) and the concentration of gel electrophoresis-purified DNA fragment was determined by an Eppendorf BioPhotometer (Germany).

2.3. Electropolymerization of 1,5-naphthalenediamine

GCE was polished sequentially with 0.3 and 0.05 μ m alumina (Al₂O₃) paste, and then sonicated in water, 1:1 nitric acid (HNO₃) and ethanol successively, each for 5 min. The electrode was scanned by cyclic voltammetry in 0.5 M H₂SO₄ between -0.4 V and 0.8 V (vs. SCE) at 100 mV/s until a steady state was reached. Then the electrode was employed as the working electrode and immersed in the mixture of 0.1 M HCl and 25 mM 1,5-naphthalenediamine

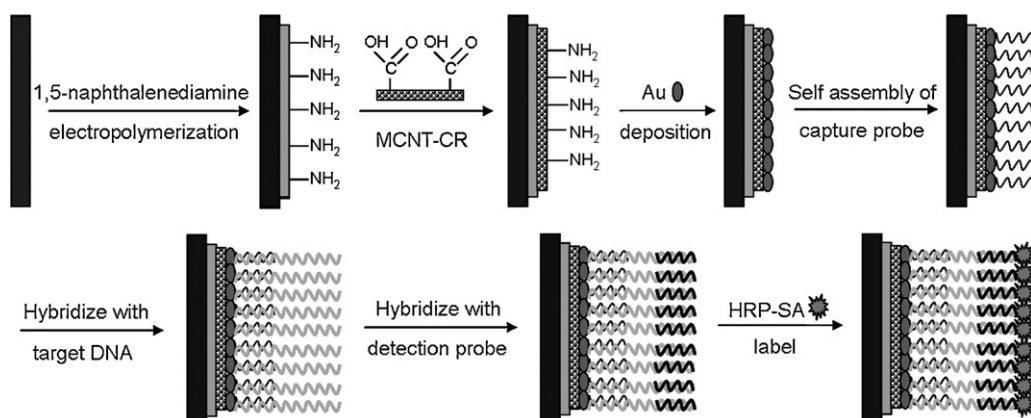


Fig. 1. Schematic diagram of the film assembly and DNA hybridization processes.

with the volume ratio of 1:1 for electropolymerization by cyclic sweeping for 5 cycles. The potential range was -0.2 V to 0.8 V (vs. Ag/AgCl) and the scan rate was 50 mV/s . The resulting poly (1,5-naphthalenediamine) film modified GCE was rinsed with water and dried naturally.

2.4. Preparation of MWCNT-CR modified electrode

The preparation of CR-functionalized water-soluble MWCNTs was carried out by using a simple physical grinding treatment according to the previously reported literatures [40,41]. Firstly, MWCNTs were carboxylated by refluxing in 2.5 M HNO_3 for 6 h and treating with 2.0 M HCl for 12 h. The carboxylated MWCNTs were thoroughly washed with water and centrifuged at 3000 rpm for 10 min, and then dried at 60°C under vacuum for 3 h before use. Secondly, the dried MWCNTs were mixed with CR on the mass ratio of 5/1 in an agate mortar and ground for 2 h with the addition of little water every now and then to avoid agglomeration of the dry CR powder. Then the product was readily dissolved in water by vigorously shaking the solution and centrifuged at 1000 rpm for 20 min. The transparent black supernatant was collected with solubility as high as 3.2 mg/mL in water and was denoted as MWCNT-CR. Thirdly, $6\text{ }\mu\text{L}$ mixture of MWCNT-CR, 5 mM EDC and 10 mM NHS was dripped onto the poly (1,5-naphthalenediamine) modified GCE and air-dried. The MWCNT-CR modified electrode was immersed into water for three times to remove excessive free materials and dried naturally.

2.5. Electrodeposition of gold nanoparticles

The MWCNTs/poly (1,5-naphthalenediamine) modified GCE was employed as the working electrode for the electrodeposition of GNPs [42], which was immersed in an aqueous solution of $0.1\text{ wt.}\%$ HAuCl_4 by cyclic potential sweeping in the potential range of $0\text{--}0.9\text{ V}$ (vs. SCE) for 3 cycles at a scan rate of 10 mV/s . The GNPs/MWCNTs/poly (1,5-naphthalenediamine) modified GCE was copiously rinsed with water and dried under nitrogen flow.

2.6. Sample preparation of CDH gene fragment from *P. chrysosporium*

P. chrysosporium cultures were grown on potato dextrose agar (PDA) at 37°C for 7 days. The spores were inoculated into potato dextrose liquid medium and incubated at 37°C with a shaking rate of 150 rpm for 72 h on a rotary shaker. The extraction of genomic DNA from mycelia of *P. chrysosporium* was the same as the method described previously [43]. PCR amplification was performed to obtain the target fragment of CDH genes for the direct hybridization

detection. Two microliters of the extracted genomic DNA was used as the template in PCR amplification performed in $50\text{ }\mu\text{L}$ amplification mixture containing 20 nM of each oligonucleotide primer, $25\text{ }\mu\text{L } 2\times\text{ Taq PCR Master Mix}$ and $19\text{ }\mu\text{L}$ deionized water. The target DNA was amplified by using an initial denaturation at 94°C for 5 min, then 94°C denaturation for 30 s, 48°C anneal for 30 s, and 72°C extension for 1 min for all subsequent 30 cycles, followed by a final extension at 72°C for 5 min. The PCR-amplified products were separated by gel electrophoresis on an agarose gel stained with bromophenol blue and SYBR Green I (Marker II was used for calibration). The target fragment of CDH was 309 bp and purified by using TIANGel Midi Purification Kit.

2.7. The immobilization of the ssDNA on the modified electrode surface

Five microliters of the thiolated capture probe ($20\text{ }\mu\text{M}$) was dropped onto the surface of GNPs/MWCNTs/poly (1,5-naphthalenediamine) modified GCE and kept at 4°C for self-assembling for 12 h. Then the electrode was copiously rinsed with Tris-HCl buffer and water to remove nonspecifically adsorbed materials. The capture probe coated electrode was soaked into 1 mM MCH solution for 1 h and thoroughly washed with Tris-HCl buffer and water.

2.8. Hybridization and electrochemical detection

The electrode was successively immersed in hybridization solutions containing the target nucleic acid and biotinylated detection probe at 37°C for 1 h, followed by washing with Tris-HCl buffer and water. Afterwards, it was incubated into phosphate buffer saline (PBS, pH 6.98) containing HRP-SA ($2\text{ }\mu\text{g/mL}$) at 37°C for 30 min. The HRP labeled electrode was scanned by cyclic voltammetry in 67 mM PBS (pH 6.98) containing 5 mM hydroquinone in the potential range of -0.8 V to 0.8 V (vs. SCE) at a scan rate of 100 mV/s . A pair of well-defined redox peaks was obtained and the potential of the reduction peak was used as the working potential. The chronoamperometry was performed at the constant working potential of -0.04 V (vs. SCE). The change of current vs. time catalyzed by HRP was measured with the addition of $1\text{ mM H}_2\text{O}_2$ under sustained stirring. The rapid increase of the reduction current implied the capture of HRP-SA on the composite films-modified electrode. In this paper, all the reported results for every electrode were the mean value from the three parallel measurements.

The real sample of CDH target gene was applied to the DNA sensor detection as the same procedure used for synthetic oligonucleotide. The PCR product of CDH gene from *P. chrysosporium* was denatured by heating to 94°C for 5 min, then immediately chilled

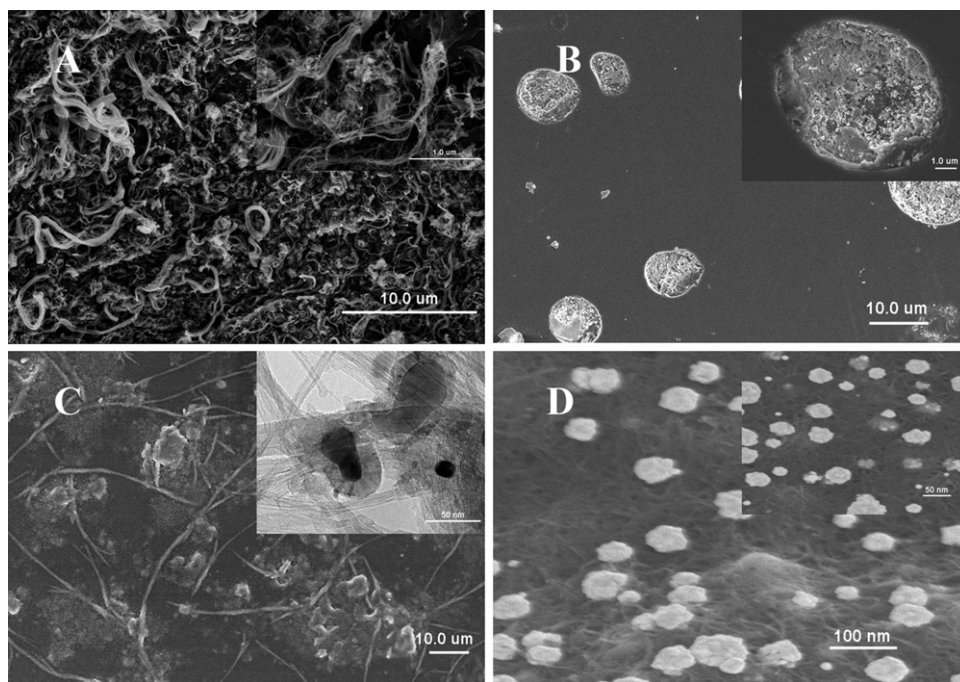


Fig. 2. SEM images of different films modified electrode: (A) raw MWCNTs, inset is the high-resolution image; (B) poly (1,5-naphthalenediamine)/GCE, inset is the high-resolution image; (C) MWCNT-CR/poly (1,5-naphthalenediamine)/GCE, inset is the TEM image; (D) GNPs/MWCNT-CR/poly (1,5-naphthalenediamine)/GCE, inset is the high-resolution image.

into ice for 30 s to obtain the target ssDNA [44,45]. The concentration of the CDH target gene fragment was also measured by UV spectrometry on Eppendorf BioPhotometer for comparison.

3. Results and discussion

3.1. The fabrication principles of the DNA sensor

The schematic diagram of the film assembly and DNA hybridization processes was illustrated in Fig. 1. The poly (1,5-naphthalenediamine) was electropolymerized on the bare GCE surface with numerous free amino groups. MWCNTs were carboxylated by treating with HNO_3 and HCl , and the solubility of MWCNTs in water was greatly improved by the interaction with CR. With the covalent bonding of amino and carboxyl groups, the casting of MWCNTs-CR solution on the poly (1,5-naphthalenediamine) modified electrode was accomplished by a protocol of EDC and NHS. Therefore, the compact MWCNT-CR film was rather firmly attached to the electrode surface and hard to be wiped off neither in the dry state nor in the electrolyte solution. Meanwhile, the high-density CR molecules decorated MWCNTs could create plenty of binding sites (i.e., the amino groups of CR) for the adsorption and accumulation of HAuCl_4 . The electrodeposition of GNPs on the MWCNTs/poly (1,5-naphthalenediamine) modified electrode could optimize the performance of the sensor and reduce or even eliminate the valence band barrier of MWCNTs in the process of electron transport. The continuous GNPs film together with the MWCNT-CR film largely increased the surface area, conductivity and electrocatalytic activity, and significantly improved the sensitivity of DNA detection. The capture probes with thiol groups were easily immobilized onto the GNPs/MWCNTs/poly (1,5-naphthalenediamine) modified GCE surface by a direct formation of thiol–Au bond. The target DNA sequences were captured by the complementary thiol-probes during the first hybridization. Then the biotinylated detection probes were introduced to the surface during the secondary hybridization and the HRP–SA conjugates were labeled to the detection probes through biotin–avidin bond. The electrode was immersed

into solution containing the substrate of HRP, and the electrochemical detection was carried out through the catalyzed reaction.

3.2. Surface morphology of different modified films

Fig. 2 shows the scanning electron microscopy (SEM) images for the different films modified electrode. Obviously, raw MWCNTs are assembled into bundles or ropes with diameters varying in a wide range, which are tangled together to form disordered network structures (Fig. 2A). As shown in Fig. 2B, under the optimum experimental conditions, the thickness of the poly (1,5-naphthalenediamine) film is about 5–7 μm . The poly (1,5-naphthalenediamine) layer is made up of uniform large sphere particles of about 7 μm in diameter, potentially due to aggregation of 1,5-naphthalenediamine monomer during electropolymerization. With the noncovalent functionalization by CR, MWCNTs were readily dissolved in water with high solubility and formed the compact, uniform and stable network nanostructures (Fig. 2C). The inset figure of Fig. 2C is the transmission electron microscopy (TEM) image of CR-modified MWCNT which is in accordance with the SEM image and exhibits the morphology characterization of MWCNT-CR. The electrodeposition in the aqueous solution of HAuCl_4 by cyclic potential sweeping led to the formation of a dense and continuous GNPs thin film on the MWCNT-CR/poly (1,5-naphthalenediamine) modified electrode. The high-resolution image revealed that the GNPs film comprised of numerous spheres of about 50 nm (Fig. 2D). It was clear that the three-step procedure for the surface modification greatly improved the performance of the sensor and facilitated its practical application in electroanalysis.

3.3. Electrochemical characterization of the DNA sensor

The features of electrode surface in the process of modification can be followed by electrochemical impedance spectroscopy of ferro/ferricyanide solutions. Fig. 3 represents the Nyquist plot of impedance for differently modified electrode in 0.1 M KCl solution containing 5.0 mM $[\text{Fe}(\text{CN})_6]^{3-/4-}$ at the scan rate of 100 mV/s vs.

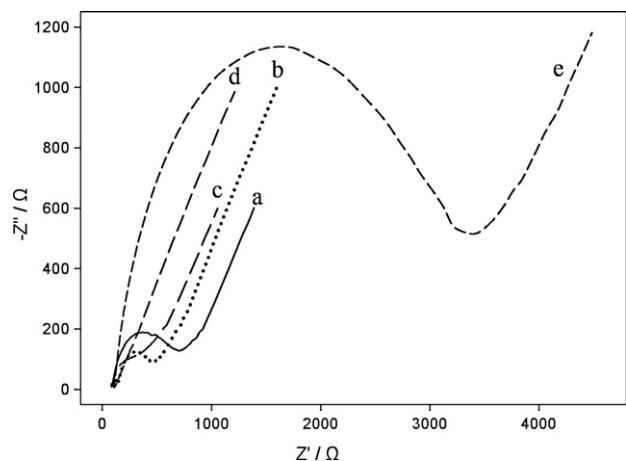


Fig. 3. Electrochemical impedance spectra of bare GCE (a); poly (1,5-naphthalenediamine)/GCE (b); MWCNT-CR/poly (1,5-naphthalenediamine)/GCE (c); GNPs/MWCNT-CR/poly (1,5-naphthalenediamine)/GCE (d); dsDNA/GNPs/MWCNT-CR/poly (1,5-naphthalenediamine)/GCE (e), using a 0.1 M KCl solution containing 5.0 mM ferro/ferricyanide solution, with frequency range of 0.01–10⁵ Hz, a bias potential of 0.20 V vs. SCE and an AC amplitude of 5 mV.

SCE. The interfacial electron-transfer resistance (R_{et}) for bare GCE and 1,5-naphthalenediamine/GCE were 632 Ω (curve a) and 560 Ω (curve b), respectively. After the modification of MWCNTs, the value of R_{et} decreased to 380 Ω (curve c), which could be ascribed to the fact that the high conductivity of MWCNTs accelerated the electron transfer on the electrode. An almost straight line was observed for the assembly of gold nanoparticles on the MWCNTs modified GCE (curve d), indicating that the introduction of GNPs could improve the electron transfer kinetic to a large extent. After immobilization of capture probe and hybridization of target complementary ssDNA, the value of R_{et} was increased to 3218 Ω (curve e). Electron transfer became more difficult because of the introduction of probe DNA and target ssDNA resulting in negative charge enhancement on the electrode surface.

The cyclic voltammograms of ferro/ferricyanide solutions through the modified electrode could be used as a valuable tool to provide information on the interfacial conformation. Fig. 4 shows the cyclic voltammograms obtained for differently modified electrode in 0.1 M KCl solution containing 5.0 mM $[\text{Fe}(\text{CN})_6]^{3-/4-}$ at

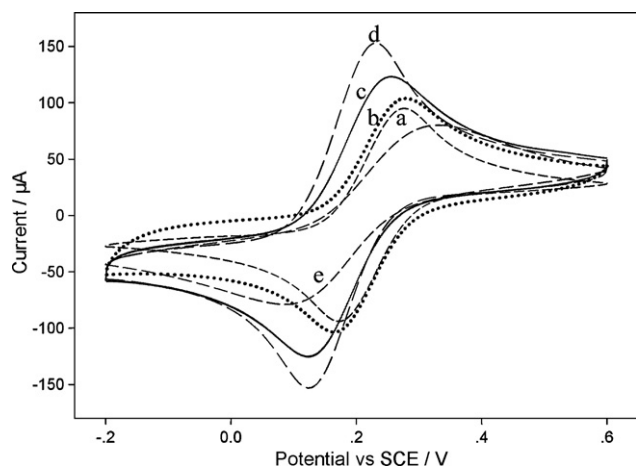


Fig. 4. Cyclic voltammograms of bare GCE (a); poly (1,5-naphthalenediamine)/GCE (b); MWCNT-CR/poly (1,5-naphthalenediamine)/GCE (c); GNPs/MWCNT-CR/poly (1,5-naphthalenediamine)/GCE (d); dsDNA/GNPs/MWCNT-CR/poly (1,5-naphthalenediamine)/GCE (e), using a 0.1 M KCl solution containing 5.0 mM ferro/ferricyanide solution, with potential range of -0.2 to 0.6 V (vs. SCE), and a scan rate of 100 mV/s.

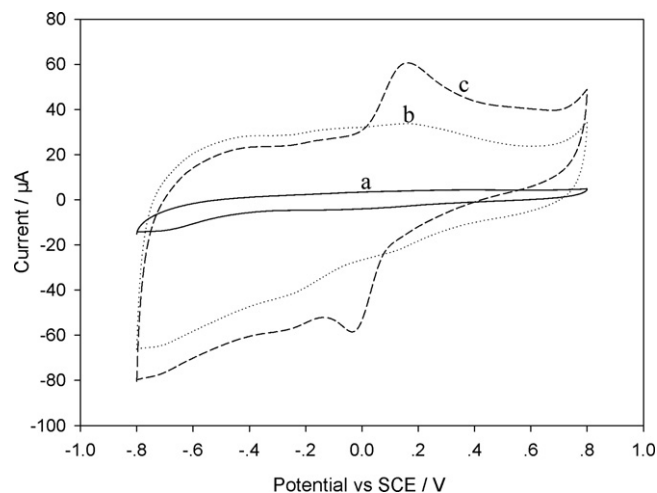


Fig. 5. Cyclic voltammograms of bare GCE in blank PBS (a); dsDNA/GNPs/MWCNT-CR/poly (1,5-naphthalenediamine)/GCE in blank PBS (b); dsDNA/GNPs/MWCNT-CR/poly (1,5-naphthalenediamine)/GCE in PBS containing 0.1 M hydroquinone and 0.1 M H_2O_2 (c), using a 67 mM PBS (pH 6.98) in the potential range of -0.8 V to 0.8 V (vs. SCE) at a scan rate of 100 mV/s.

the scan rate of 100 mV/s vs. SCE. As was shown in the figure, the polymerization of 1,5-naphthalenediamine was evidenced by a slight increase in the voltammetric response of $[\text{Fe}(\text{CN})_6]^{3-/4-}$ (curve b) than that of bare electrode (curve a) and the peak current of $[\text{Fe}(\text{CN})_6]^{3-/4-}$ was increased obviously with the modification of MWCNT-CR (curve c), which inferred that the rate of electron transfer of MWCNT-CR was faster than poly (1,5-naphthalenediamine). The assembly of gold nanoparticles on MWCNT-CR/poly (1,5-naphthalenediamine)/GCE was convinced to increase the effective electrode surface area and enhance the electron transfer rate, which was evidenced by a largest increase in the voltammetric response of $[\text{Fe}(\text{CN})_6]^{3-/4-}$ (curve d). However, when the immobilization of capture probe and hybridization of target complementary ssDNA proceeded, the peak current of $[\text{Fe}(\text{CN})_6]^{3-/4-}$ was observed with a significant decrease (curve e). The introduction of probe DNA and complementary DNA increased the negative charge which is responsible for the increased repulsion of redox species. The results by cyclic voltammetric experiment were consistent with the detection by impedance experiment, which revealed that the DNA immobilization and hybridization could be effectively operated on the fabricated electrode surface.

The cyclic voltammograms obtained for differently modified electrode in 67 mM PBS (pH 6.98) in the potential range of -0.8 V to 0.8 V (vs. SCE) at a scan rate of 100 mV/s is shown in Fig. 5. It could be observed that a low background current of bare GCE was obtained in blank PBS (curve a). After immobilization and hybridization on the composite films-modified electrode, the background current was higher and no obvious peaks displayed in the absence of hydroquinone (curve b). With the addition of 0.1 M H_2O_2 to the buffer solution containing 0.1 M hydroquinone, a pair of well-defined redox peaks appeared according to the reduction of quinone species produced by HRP-catalyzed hydroquinone oxidation on the surface of electrode (curve c). The result fully illustrated the successful immobilization of probe DNA and target ssDNA by nucleic acid hybridization.

3.4. Optimization of experimental conditions

3.4.1. Effect of the concentration and scan rate of 1,5-naphthalenediamine

Both the concentration and scan rate of 1,5-naphthalenediamine are important to obtain a compact and uniform polymer film which directly influence the electron

transfer rate and the maximum loading amount of MWCNTs. Fig. S1(A) (supplementary data) displays the cyclic voltammograms recorded for different concentrations of 1,5-naphthalenediamine in HCl electrolytic solution at the scan rate of 50 mV/s. As can be seen, well defined redox peak height of polymer increased with increasing volume ratios of 25 mM 1,5-naphthalenediamine and 0.1 M HCl in 1:3, 1:2 and 1:1. However, when the volume ratios of 1,5-naphthalenediamine and HCl further increased in 2:1 and 3:1, the height of peaks for polymerization of 1,5-naphthalenediamine were decreased obviously. This revealed that higher concentrations of 1,5-naphthalenediamine monomer play an important role in formation of free radical cationic polymerization which controlled the diagram and thickness of the polymer film. Nevertheless, the redox behavior of the polymer film was also dependent on the pH of the HCl electrolyte solution. Consequently, the volume ratio of 1:1 was selected as the optimum concentration for electropolymerization.

Cyclic voltammograms of bare GCE at the various scan rates in 0.05 M HCl solution containing 12.5 mM 1,5-naphthalenediamine were investigated. As shown in Fig. S1(B) (supplementary data), a well pair of redox peak was exhibited which proved that the oxidation of 1,5-naphthalenediamine monomer occurs on the electrode. With increasing the potential scan rate from 20 to 80 mV/s, the redox peak increased gradually, suggesting that the higher scan rate of potential accelerated the electron transfer rate for polymerization of 1,5-naphthalenediamine in acidic electrolyte solution. However, in order to obtain the homogenous and uniform polymer film, 50 mV/s was chosen as the optimum scan rate for electropolymerization.

3.4.2. Effect of the coverage of MWCNT-CR

The relationship between the oxidation peak current response and the coverage of water-soluble MWCNT-CR solution was investigated by cyclic voltammogram of ferro/ferricyanide solution. Fig. S2 (supplementary data) displayed that the oxidation peak current responses increased markedly when the coverage of MWCNT-CR rose from 91 to 274 $\mu\text{g}/\text{cm}^2$. However, further increase the coverage of MWCNT-CR, the oxidation peak current responses decreased slightly, for the thicker film of MWCNT-CR blocked the electrical conductivity. Thus, the MWCNT-CR 2 coverage with 274 $\mu\text{g}/\text{cm}^2$ was employed to modify the electrode.

3.4.3. Effect of the gold electrodeposition time

The amount and particle size of the gold nanoparticles depended on the electrodeposition time. As shown in Fig. S3 (supplementary data), the change of reduction current responses increased gradually as deposition time increased. However, when increasing the gold deposition time continuously, the reduction current remained and then decreased slightly, which might be associated with the decrease of the real surface area resulting from the aggregation of GNPs on the electrode surface. So, cyclic potential sweeping of 3 cycles was selected in this work.

3.4.4. Effect of self-assembling and hybridization conditions

The coverage density of the self-assembled probes has a great influence on the sensitivity of sensor. Generally, the coverage density increases with the increasing assembly time. The effect of immobilization time on the change of reduction current response was studied. The current responses increased fast in the first 4 h and the steady state was reached after 8 h which corresponded to the saturated coverage of the capture probes, shown in Fig. S4(A) (supplementary data). Therefore, 8 h of self-assembling time was selected throughout our experiments.

Subsequent studies indicated that the hybridization temperature and hybridization time also acted as very important parameters. The hybridization efficiency was higher with the

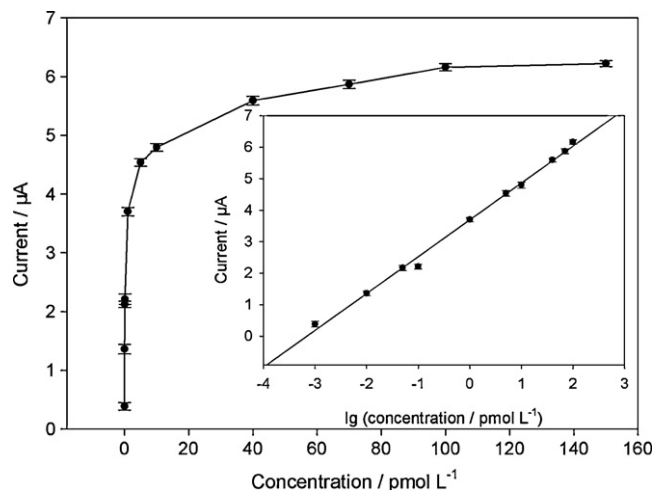


Fig. 6. Relationship between the current response and DNA concentration under the optimal experimental conditions. Inset: linear regression of current response vs. the common logarithm of target DNA concentration. The vertical bars designate the standard deviations for the means of three replicative tests.

increasing temperature before 37 °C, then the change of reduction current responses declined at higher temperatures, shown in Fig. S4(B) (supplementary data). The hybridization amount rose rapidly with time between 20 and 60 min and showed a leveling off after 60 min, exhibited in Fig. S4(C) (supplementary data). Thus, the optimal hybridization temperature was selected as 37 °C and the optimal hybridization time as 60 min.

3.5. Amperometry performance for the detection of synthesized oligonucleotide

Fig. 6 displays the calibration of response current and the concentration of CDH synthesized target oligonucleotide by chronoamperometry. As the concentration of nucleic acid increased, the HRP catalyzed reduction current increased gradually. The response current increased linearly with the common logarithm of the target ssDNA concentration in the range of 1.0×10^{-15} – 1.0×10^{-10} M, which is the appropriate concentration range to be applied for the accurate determination of DNA. The lower detection limit was 1.2×10^{-16} M ($S/N=3$), which resulted in a current signal that equaled the mean value of background signals plus three times standard deviation of background signals. The mean current value and the standard deviation of the background signals are 8.7×10^{-8} A and 1.2×10^{-8} A, respectively. The corresponding regression equation was as follows, and the correlation coefficient was 0.996.

$$I/\mu\text{A} = 1.1685 \lg(C/\text{pM}) + 3.6966 \quad (1)$$

The sensitivity of the electrochemical hybridization assay was further investigated by comparing the value of the calibration slope in this experiment with those from other similar sensor configuration. The higher sensitivity obtained from our experiment was comparable to the recently reported value of the calibration slope obtained by the sensor with similar configuration [31]. The calibration slopes of the sensors proposed in this paper and Ref. [31] are 1.1685 and 0.8112, respectively, which exhibited that the composite film modified electrode in our experiment could obtain higher sensitivity and lower detection limit.

3.6. Selectivity of DNA detection

The selectivity of the biosensor was evaluated by analyzing fully complementary and two-base-mismatched sequences under

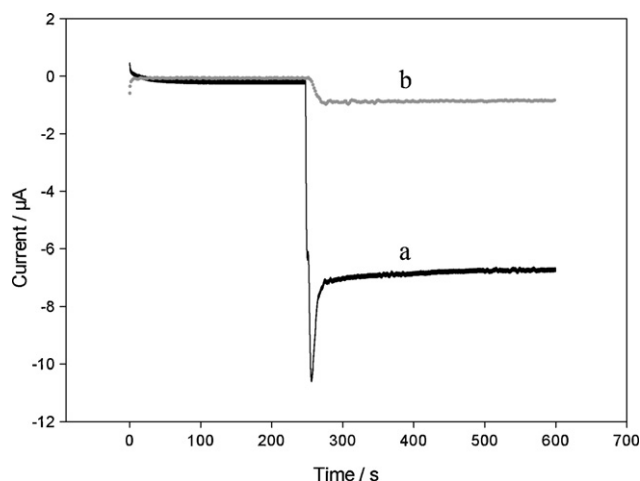


Fig. 7. The current responses of (a) complementary target ssDNA and (b) two base mismatched ssDNA, with concentration of 2×10^{-10} M in 67 mM PBS (pH 6.98) containing 0.1 M hydroquinone and 0.1 M H_2O_2 .

the same condition shown in Fig. 7. The concentration of target complementary sequence and two-base-mismatched sequence was 2×10^{-10} M. The current responses were 6.8×10^{-6} A (curve a) and 8.6×10^{-7} A (curve b), respectively. Compared with the fully complementary sequence, the current response of two-base-mismatched sequence was reduced to 13%. This exhibited a good discrimination between complementary and mismatched oligonucleotide.

3.7. Reproducibility and stability of the DNA sensor

The repeatability of the sensor was examined by determination of the same DNA concentration of three consecutive. The average of the relative standard deviations (R.S.D.) was 3.1%, which guaranteed the precision of the biosensor. The reproducibility tests using different DNA sensors were also performed with the measurement of composite films-modified electrode in 2.0×10^{-13} M target DNA solution. Three DNA sensors, made independently, showed the response current values of 2.82×10^{-6} A, 2.94×10^{-6} A and 2.76×10^{-6} A with an acceptable variation coefficient of 3.9% ($n=3$). The stability of the composite films-modified sensor before the immobilization of DNA was performed. The electrode could use many times for DNA sensors when the same GNPs/MWCNTs/poly (1,5-naphthalenediamine)/GCE was stored at 4 °C for three weeks, and it retained about 90% of its initial response. The stability of the immobilized DNA probes on electrode was investigated as well. The amperometric response of the capture probe modified electrode to target DNA retained 84% of the initial response after 15-day storage at 4 °C, which indicated the good stability of the biosensor.

3.8. Detection of CDH gene sample

The denatured ssDNA of CDH fragments from *P. chrysosporium* genomic DNA was applied to the DNA sensor detection after PCR amplification. The gel electrophoresis photos of extracted genomic DNA and PCR product of CDH genes can be found in Fig. S5 (supplementary data). It shows that the genomic DNA of 23,000 bp (Fig. S5(A)) and the target fragments of CDH (309 bp, Fig. S5(B)) were successfully extracted with high purity by adopting the proposed method and appropriate PCR amplification protocol. With the same procedure used for the synthetic oligonucleotide, different concentrations of solution containing the target 309 bp CDH gene (shown in Fig. S6, supplementary data) were determined by the current fabricated biosensor and UV spectrometry

Table 2

The detection results of CDH fragment sample from *P. chrysosporium* by the DNA sensor and UV spectrometry.

Concentration calibrated by UV spectrometry ($\mu\text{mol L}^{-1}$)	Average concentration recovered by DNA sensor ^a ($\mu\text{mol L}^{-1}$)	CV (%)	Recovery (%)
1.35	1.22 ± 0.14	11.47	90.37
6.72	7.06 ± 0.38	5.38	105.06
17.28	16.09 ± 1.25	7.76	93.11
25.96	27.53 ± 1.54	5.59	106.05
34.88	32.35 ± 2.56	7.91	92.75
45.63	42.51 ± 3.19	7.50	93.16
52.12	55.83 ± 3.67	6.57	107.12
60.92	64.74 ± 4.02	6.21	106.27
78.81	73.85 ± 5.21	7.05	93.71
86.73	81.68 ± 5.23	6.40	94.18

^aAverage values and standard deviations of three replicates.

(260 nm wavelength), and the results of the two methods were approximately the same, displayed in Table 2. This proved that the biosensor offered a simple, fast and sensitive method for DNA detection with favorable accuracy and specificity.

4. Conclusion

An electrochemical sensor based on GNPs/MWCNTs/poly (1,5-naphthalenediamine) was developed. The GNPs and MWCNTs could significantly enhance the DNA immobilization and electrocatalytic activity with excellent conductivity and large surface area. The film assembly and DNA hybridization processes were investigated by scanning electron microscopy, electrochemical impedance spectroscopy and cyclic voltammetry. The amperometric current response was linearly related to the common logarithm of the target nucleic acid concentration in the range of 1.0×10^{-15} – 1.0×10^{-10} M, with the detection limit of 1.2×10^{-16} M. Because of the superior sensitivity and selectivity, the composite films-modified electrode has been applied for the detection of cellobiose dehydrogenase gene from *P. chrysosporium* with HRP label which induced the signal amplification. The PCR amplification was demonstrated to be a valuable strategy for obtaining sensitive and accurate diagnosis of DNA sample. The electrochemical detection results of real samples from *P. chrysosporium* genomic DNA were in good agreement with UV spectrometry, while the method of biosensor was more convenient, rapid and sensitive. This sensor based on nanocomposite modification could be used for the detection of bioactive substances and offered a possible method for “on-the-spot” monitoring in life sciences, clinical medicine and environmental pollution control systems.

Acknowledgements

The study was financially supported by the Fundamental Research Funds for the Central Universities, the National Natural Science Foundation of China (50608029, 50978088, 50808073, 51039001), the Program for Changjiang Scholars and Innovative Research Team in University (IRT0719), the Hunan Key Scientific Research Project (2009FJ1010) and the Hunan Provincial Natural Science Foundation of China (10JJ7005).

Appendix A. Supplementary data

Supplementary data associated with this article can be found, in the online version, at doi:10.1016/j.electacta.2011.03.035.

References

- [1] M. Tuomela, M. Vikman, A. Hatakka, M. Itävaara, *Bioresour. Technol.* 72 (2000) 169.
- [2] S. Shleev, P. Persson, G. Shumakovich, Y. Mazhugo, A. Yaropolov, T. Ruzgas, L. Gorton, *Enzyme Microb. Technol.* 39 (2006) 835.
- [3] D. Cullen, *J. Biotechnol.* 53 (1997) 273.
- [4] P. Kersten, D. Cullen, *Fungal Genet. Biol.* 44 (2007) 77.
- [5] S.D. Mansfield, E. DeJong, J.N. Saddler, *Appl. Environ. Microbiol.* 63 (1997) 3804.
- [6] L. Hildén, G. Johansson, G. Pettersson, J.B. Li, P. Ljungquist, G. Henriksson, *FEBS Lett.* 477 (2000) 79.
- [7] M.D. Cameron, S.D. Aust, *Enzyme Microb. Technol.* 28 (2001) 129.
- [8] G. Henriksson, G. Johansson, G. Pettersson, *J. Biotechnol.* 78 (2000) 93.
- [9] T. Kajisa, M. Yoshida, K. Igarashi, A. Katayama, T. Nishino, M. Samejima, *J. Biosci. Bioeng.* 98 (2004) 57.
- [10] S.S. Subramaniam, S.R. Nagalla, V. Renganathan, *Arch. Biochem. Biophys.* 365 (1999) 223.
- [11] U. Baminger, B. Nidetzky, K.D. Kulbe, D. Haltrich, *J. Microbiol. Methods* 35 (1999) 253.
- [12] G. Henriksson, G. Pettersson, G. Johansson, A. Ruiz, E. Uzategui, *Eur. J. Biochem.* 196 (1991) 101.
- [13] B.P. Roy, F.S. Archibald, *Anal. Biochem.* 216 (1994) 291.
- [14] C.F. Ding, F. Zhao, M.L. Zhang, S.S. Zhang, *Bioelectrochemistry* 72 (2008) 28.
- [15] X. Mao, J.H. Jiang, X.M. Xu, X. Chu, Y. Luo, G.L. Shen, R.Q. Yu, *Biosens. Bioelectron.* 23 (2008) 1555.
- [16] L. Tang, G.M. Zeng, J.X. Liu, X.M. Xu, Y. Zhang, G.L. Shen, Y.P. Li, C. Liu, *Anal. Bioanal. Chem.* 391 (2008) 679.
- [17] L. Tang, G.M. Zeng, G.L. Shen, Y.P. Li, Y. Zhang, D.L. Huang, *Environ. Sci. Technol.* 42 (2008) 1207.
- [18] L. Tang, G.M. Zeng, G.L. Shen, Y. Zhang, G.H. Huang, J.B. Li, *Anal. Chim. Acta* 579 (2006) 109.
- [19] Y. Zhang, G.M. Zeng, L. Tang, D.L. Huang, X.Y. Jiang, Y.N. Chen, *Biosens. Bioelectron.* 22 (2007) 2121.
- [20] P. Du, H.X. Li, Z.H. Mei, S.F. Liu, *Bioelectrochemistry* 75 (2009) 37.
- [21] Y.C. Tsai, S.C. Li, S.W. Liao, *Biosens. Bioelectron.* 22 (2006) 495.
- [22] J.M. Pingarrón, P. Yáñez-Sedeño, González-Cortés, *Electrochim. Acta* 53 (2008) 5848.
- [23] I. Capek, *Adv. Colloid Interface Sci.* 150 (2009) 63.
- [24] A.V. Ellis, K. Vijayamohan, R. Goswami, N. Chakrapani, L.S. Ramanathan, P.M. Ajayan, G. Ramanath, *Nano Lett.* 3 (2003) 279.
- [25] F. Valentini, A. Amine, S. Orlanducci, M.L. Terranova, G. Palleschi, *Anal. Chem.* 75 (2003) 5413.
- [26] M.L. Pedano, G.A. Rivas, *Electrochem. Commun.* 6 (2004) 10.
- [27] R.R. Moore, C.E. Banks, R.G. Compton, *Anal. Chem.* 76 (2004) 2677.
- [28] W. Sun, P. Qin, H.W. Gao, G.C. Li, K. Jiao, *Biosens. Bioelectron.* 25 (2010) 1264.
- [29] J.A. Ribeiro, C.A. Carreira, H.J. Lee, F. Silva, A. Martins, C.M. Pereira, *Electrochim. Acta* 55 (2010) 7892.
- [30] O.A. Sadik, S.K. Mwilu, A. Aluoch, *Electrochim. Acta* 55 (2010) 4287.
- [31] J. Wang, S.P. Li, Y.Z. Zhang, *Electrochim. Acta* 55 (2010) 4436.
- [32] Y.J. Guo, S.J. Guo, Y.X. Fang, S.J. Dong, *Electrochim. Acta* 55 (2010) 3927.
- [33] F. Xiao, F.Q. Zhao, J.W. Li, L.Q. Liu, B.Z. Zeng, *Electrochim. Acta* 53 (2008) 7781.
- [34] X.C. Deng, F. Wang, Z.L. Chen, *Talanta* 82 (2010) 1218.
- [35] J.H. Lin, C.Y. He, L.J. Zhang, S.S. Zhang, *Anal. Biochem.* 384 (2009) 130.
- [36] Z.Y. Lin, L.Z. Huang, Y. Liu, J.M. Lin, Y.W. Chi, G.N. Chen, *Electrochem. Commun.* 10 (2008) 1708.
- [37] M.N. Zhang, L. Su, L.Q. Mao, *Carbon* 44 (2006) 276.
- [38] Z.J. Wang, M.Y. Li, Y.J. Zhang, J.H. Yuan, Y.F. Shen, L. Niu, A. Ivaska, *Carbon* 45 (2007) 2111.
- [39] Y.Z. Zhang, H.Y. Ma, K.Y. Zhang, S.J. Zhang, J. Wang, *Electrochim. Acta* 54 (2009) 2385.
- [40] C.G. Hu, Z.L. Chen, A.G. Shen, X.C. Shen, J. Li, S.S. Hu, *Carbon* 44 (2006) 428.
- [41] C.G. Hu, C.H. Yang, S.S. Hu, *Electrochem. Commun.* 9 (2007) 128.
- [42] C.G. Hu, Y. Ding, Y.P. Ji, J.H. Xu, S.S. Hu, *Carbon* 48 (2010) 1345.
- [43] L. Tang, G.M. Zeng, G.L. Shen, Y.P. Li, C. Liu, Z. Li, J. Luo, C.Z. Fan, C.P. Yang, *Biosens. Bioelectron.* 24 (2009) 1474.
- [44] K. Arora, N. Prabhakar, S. Chand, B.D. Malhotra, *Anal. Chem.* 79 (2007) 6152.
- [45] P. Kara, S. Cavdar, A. Berdeli, M. Ozsoz, *Electroanalysis* 19 (2007) 1875.